Title: Beyond G1/S regulation: how cell size homeostasis is tightly controlled throughout the cell cycle?

Short title: cell size homeostasis is tightly controlled throughout the cell cycle

Author: Xili Liu[1], Jiawei Yan[2], Marc W. Kirschner[1, *]

[1]Department of Systems Biology, Harvard Medical School, Boston, MA 02115

[2]Department of Chemistry, Stanford University, Stanford, CA 94305

[*]corresponding author: marc@hms.harvard.edu

Authors contribution

X.L. and M.W.K. designed research; X.L. performed research; X.L. analyzed data; X.L. and J.Y. built the stochastic models. X.L and M.W.K. wrote the paper.

Abstract

Proliferating cells require control mechanisms to counteract stochastic noise and stabilize the cell mass distribution in a population. It is widely believed that size-dependent timing of the G1/S transition is the predominant control process in mammalian cells. However, a model based only on such a checkpoint cannot explain why cell lines with deficient G1/S control are still able to maintain a stable cell mass distribution or how cell mass is maintained throughout the subsequent phases of the cell cycle. To answer such questions, we used a recently developed form of Quantitative Phase Microscopy (ceQPM), which provides much-improved accuracy of individual cell mass measurement, to investigate the factors contributing to cell mass homeostasis. We find that cell mass homeostasis is robustly maintained, despite disruptions of the normal G1/S transition or cell growth rate. The coefficient of variation in mass, nevertheless declines well after the G1/S transition and throughout the cell cycle in both transformed and non-transformed cells. Furthermore, the cell growth rate responds to cell mass in different ways in different cell types. Growth rate modulation is conveyed by mTORC1-dependent and mTORC1-independent processes, which are independently regulated. Slightly reduced mass accumulation, below exponential growth can effectively reduce cell mass variation in a population. Both size-dependent cell cycle regulation and size-dependent growth rate modulation contribute to cell mass homeostasis. Together they form a compensatory network that strictly controls the coefficient of variation of cell mass in a population. These findings opens new avenues for the discovery of underlying molecular mechanisms. Furthermore, understanding feedback directly on cell growth may provide insights into fundamental principles of cell size control in normal proliferating and terminally differentiated cells, as well as cells in pathological circumstances.

Introduction

The distribution of cell size in a population of proliferating cells is very accurately maintained over many generations despite variability of the rate of cell growth, variability of the period of the cell cycle, and the imprecision in the equipartition of daughter cells at mitosis. Each of these factors contributes to the dispersion of cell size in the population(1). It was self-evident that there had to be some “correction” mechanism that would act within individual cells to counteract the combined effects of random variation, in order to ensure a stable size distribution in the population. This problem has been appreciated for a long time(2). For the most part, studies on mammalian and yeast cell size homeostasis have been focused on size-dependence of the G1 length: small cells spend a longer time in the G1 phase to catch up with larger cells, thus reducing size variability at S phase entry(2–8). Several molecular players of this process have been identified, such as the dilution of retinoblastoma (Rb) protein(6,9) and the activation of p38 MAPK kinase(10,11). However, as effective as such a single mechanism might be, it cannot account for the constancy in the cell size distribution. Specifically, if G1 length regulation were the only working mechanism, cells would not be able to control any extensive variation introduced during the nonG1 phases, which collectively occupy a larger portion of the cell cycle than G1 in many cell types. Furthermore, proliferating cells seem to find a way to achieve size homeostasis, no matter what their surrounding environment and genetic background are(12). Such robustness could suggest that size homeostasis may be maintained by more than one mechanism.

In 1985, Zetterberg et al. found that the variation of G1 length accounted for most of the variation in cell cycle length when cells switched from quiescence to proliferation (13). However, a later study

discovered that the G1, S, and G2 phase lengths had comparable variability and were all positively correlated with the cell cycle length in normal cycling populations (14), implying a dependency on cell size outside of G1. Regulation of the S and G2 lengths are known to make a contribution to size homeostasis in lower eukaryotic organisms, such as budding and fission yeasts(15–17). Evidence of size-dependent regulation outside of G1 has seldom been reported in mammalian cells(4,7). Little is known about whether the nonG1 phases play a role in maintaining mammalian cell size homeostasis or whether the size variation added in the nonG1 phases is somehow compensated fully at the next G1/s transition. It is also unclear whether the nonG1 phases contribute to the reduction of cell size variation.

An alternative to *cell cycle* regulation for maintaining the cell size distribution is to regulate *cell growth* (1,18). Previous studies implied various types of growth rate modulation. For instance, the slope of growth rate vs. size decreases for large cells at birth(7); growth is roughly linearly (rather than exponentially) related to size for excessively large cells(19); and cell size is negatively correlated with subsequent growth rate twice during the cell cycle(8). Though these relationships have been noted, little is known about the control mechanisms underlying such complex behaviors. Fundamental questions about cell growth control, as opposed to cell cycle control, have barely been raised, such as whether mammalian cell types that undergo limited numbers of divisions would need to modulate their growth rate at all and to what degree the process of growth rate regulation contributes to cell size homeostasis.

In keeping with a preceding study in bacteria, we suggest explicitly distinguishing “size control” from “size homeostasis”(20). We refer to “size control” as the control of the mean size, as a cell responds to a change of environment; “size homeostasis” would then refer to the control on the variance around the mean size in a steady-state condition. The two concepts are closely related but different, with the latter emphasizing balanced noise and correction. We focused on cultured cell lines in this study, because primary cells may take a long time to reach a stable cell size, as they adapt to the culture conditions, and because it may be hard to ensure a steady and homogeneous environment for *in vivo* systems. However, whatever the limitations, the underlying cellular mechanisms in cell lines have generally been found to be very similar, qualitatively if not strictly quantitatively, to the in vivo state.

There is also an ambiguity in the term “cell size” that needs to be clarified before we begin. Cell size can be represented by either cell mass or cell volume. As cell volume is a more passive responder to the mechanical and osmotic signals during the cell cycle and differentiation(21–24), we prefer to focus on cell mass homeostasis in this study. Nevertheless, the lack of accurate means of measurement cell mass had thwarted the study of cell mass homeostasis and growth rate regulation in mammalian cells for decades. Measuring the mass of a single cell is surprisingly difficult, and accurately determining the growth rate from the time derivative of mass is even more challenging (25,26). In fact cell mass has been best studied to high precision for cells in suspension(27). However, for most mammalian cells the appropriate format for physiological, developmental and pathological study is for cells attached to a substratum. To study mass growth regulation of attached cells precisely enough to distinguish different models of control, requires improved methods. We recently developed computational enhanced Quantitative Phase Microscopy (ceQPM), which measures cell dry mass (the cell’s mass excluding water) to an error of less than 2% (28). To discern general features of cell mass and growth rate regulation we tracked single-cell growth and the timing of cell cycle events at a scale of thousands of cells per experiment. By using this improved technology, we could satisfactorily investigate the process of cell mass accumulation relative to cell cycle progression and derive new understandings of cell mass homeostasis during the cell cycle.

Results

Cell size variation is tightly controlled regardless of the status of the G1/S circuitry.

"Cell mass homeostasis" has a strict definition: a population of proliferating cells should maintain a stable distribution of cell mass over generations. This requires that cell mass variability, which would be expected to increase super-exponentially throughout the cell cycle after mitosis (S1 Text Chapter8, Fig. S8B), must be compensated by a reduction of variability by some means during the cell cycle (Fig. 1A). Thus the coefficient of variation (CV) of division mass CV_d should be lower than the CV of birth mass CV_b, with their quantities fulfilling the equation adapted from Huh et al. (29):

$$\mathrm{CV}_b^2 = \mathrm{CV}_d^2 + Q^2 \quad (1)$$

where Q denotes the partition error, with $Q^2 = \frac{<(m_1-m_2)^2>}{<m_1+m_2>^2}$; m_1 and m_2 are the birth masses of the two sister cells, respectively. We first verified that the cells in our system were virtually at cell mass homeostasis. By monitoring the proliferation and growth of HeLa cells by ceQPM, we found that the cells were indeed at the homeostatic state, as the difference between the left- and right-hand sides of Equation 1 was negligible (Fig. 1B).

Figure 1. Cell mass variation is tightly controlled in mammalian cell lines robust to the perturbations on G1/S regulation or growth rate. (A)Schematic of how cell mass CV changes with cell cycle progression in different scenarios. (B) The left- and right-hand sides of Eq. (1) and their difference quantified in HeLa cells; in the term $\mathrm{CV}_d^2 + Q^2$, CV_d^2 is indicated in black, Q^2 is indicated in white; error bars are the standard deviation of 8 experiments. (C-F) The mean birth mass (C), birth mass CV (D), division mass CV (E), and standard deviation of Division Asymmetry (DA std.) (F) of different cell lines. (G-J) The mean birth mass (G), birth mass CV (H), division mass CV (I), and DA std. (J) of RPE-1 and U2OS cells in the control condition, 50 nM palbociclib, 100 nM rapamycin at cell mass homeostasis, or right after adding 100 ng/mL nocodazole. Error bars in (C-J) indicate the standard deviation of more than three measurements. (K-P) The profile of how cell mass CV changes with cell cycle progression at cell mass homeostasis; error bars are the standard error of CV ($CV/\sqrt{2n}$), where n is the cell number at the corresponding cell cycle stage. The identification of cell cycle stages is illustrated in Fig. S3, and the four cell cycle phases are indicated by areas shaded in different colors.

The birth mass CV indicates the stringency of size control (Fig. 1A). If G1/S control were the predominant circuitry that gates cell size, we would expect cell lines with deficient G1/S regulation to have higher birth mass variation. We compared several human cancer cell lines, carrying a variety of G1/S deficiencies, and compared them to RPE-1, a cell line with a wild-type G1/S transition (Table S1). We measured the birth and division mass CVs over a 3-hour period, focusing on the observed mitotic events. We defined Division Asymmetry, $DA = \frac{m_{1,2}}{m_1+m_2}$, with m_1 and m_2 being the birth masses of the two sister cells, and calculated the standard deviation of DA (DA std.) to quantitatively represent the fidelity of cytokinesis, as this expression is more commonly-used than the partition error Q in Eq. 1(16,30). Despite the considerable variation in cell mass among cell lines (the mean birth mass of the largest cell

line is 1.85-fold greater than the smallest) (Fig. 1C), the difference in birth mass CV is less than 1.15-fold (Fig. 1D). The division mass CV and DA Std. for these cell lines were also comparable (Fig. 1E, F).

To assess the robustness of the birth mass CV to perturbations in G1/S, we further disrupted the G1/S regulation in RPE-1 and U2OS by the CDK4/6 inhibitor, palbociclib(31). Although U2OS cells have an intact Rb protein, whose dilution was believed to regulate the G1/S transition (6), it carries deficiencies in other G1/S regulators (Table S1) and is much less sensitive to palbociclib than RPE-1, which has an intact G1/S circuitry (Fig. S1A, B). Both cell lines were examined at a low dose of palbociclib, where there was sustained proliferation(10). We measured the cells after being cultured for more than one week in palbociclib when the mass distribution of each had reached a new steady state. The mean mass at birth increased by 1.68- and 1.12-fold, respectively, in RPE-1 and U2OS cells (Fig. 1G). However, the birth mass CV of each hardly changed (0.96- and 0.97- fold compared to the control condition) (Fig. 1H). Similarly, the division mass CV and the standard deviation of division asymmetry, DA std., did not change much for both cell lines in palbociclib. (Fig. 1I, J). When we exposed these cultures to the mTOR inhibitor rapamycin, we got similar results to the palbociclib treatments. Inhibiting cell growth by rapamycin reduced the steady-state mass by 27 and 20%, respectively in RPE-1 and U2OS cells (Fig. 1G), but did not affect the birth mass CV, division mass CV, or division asymmetry (Fig. 1H-J). By contrast, when we directly perturbed division by nocodazole(32) (Fig. S2A, E) and measured the cells right after adding the drug, but before they reached the new steady state, the birth mass CV, division mass CV, and DA std. all increased dramatically by 1.26- to 1.68-fold, although the mean mass at birth did not change (Fig. 1G-J, Fig. S2B-D, F-H). The results in five different cell lines and with these drug perturbations indicated that cell mass variation is robustly maintained, and much more resistant to the changes in the mean mass, G1/S regulation, or cell growth rate.

As illustrated in Fig. 1A, if G1/S were the only “size control checkpoint”, we would expect all the cell mass CV reduction to occur before or right at the G1/S transition. Cell mass variability would then be expected to rise super-exponentially after G1/S due to the lack of any other size control processes in S or G2 (S1 Text Chapter8). Thus the CV reduction before the G1/S would have to greatly undershoot the birth mass CV to compensate for the cell mass variability that would accumulate during the S and G2 phases. But if the variability in these phases were uncorrelated to the variability in G1, there would be no way to anticipate it; hence variability in division mass should easily be perturbed. To test this prediction, we examined the profile of cell mass CV reduction *throughout* the cell cycle in four different cell lines. To define the cell cycle mean path we used DNA content and fluorescently tagged Geminin, a cell cycle protein that accumulates in S phase and is rapidly degraded in mitosis. We divided this cell cycle mean path into 13 or 14 stages, depending on the cell line (Fig. S3A) (33). Each stage had a similar number of cells, except for the first and last stages, where the markers lacked resolution. We grouped these stages using the two quantitative markers into four cell cycle phases: early G1, late G1, S, and G2-M (Fig. S3B-E). Although the mass CVs in the “birth”, “G1/S”, and “division” stages were slightly larger than the ones at exact times measured by tracking the whole cell cycle, the relative trends were consistent (Fig. S3F). The result indicates that, although the cell mass CVs of different stages on the cell cycle mean path have higher noise due to some ambiguity in timing, their trend faithfully reflects how cell mass variability changes with cell cycle progression. In RPE-1, U2OS, and HT1080 cells, we found that the cell mass CV, as expected declined in late G1 and G1/S, but surprisingly kept decreasing in S phase. The decrease in CV cannot be explained by a reduction in noise, but rather implies some kind of feedback control. In particular, in HeLa cells, the CV reduction did not occur in G1 but only took place in

the S phase. Such behavior cannot be explained by regulation at the "Restriction Point" or the G1/S transition(1,18). We also tried perturbing RPE-1 cells by rapamycin and palbociclib and measured the CV reduction profiles at the new steady states. Although the drugs altered the duration of the cell cycle phases, the intensity of the cell cycle markers were still distributed along the original cell cycle mean path (Fig. S3G, H, Table S2). This enabled us to use the cell cycle stages measured in untreated cells to assign cell cycle positions for cells treated with the drugs. We found that disrupting the G1/S transition with palbociclib made the mass CV reduction in the S phase more pronounced (Fig. 1O)! By contrast inhibiting cell growth with rapamycin made the mass CV reduction more pronounced in late G1 (Fig. 1P). Notably under both conditions, where the cell cycle is significantly delayed, size homeostasis is still maintained at a similarly stringent level (Fig. 1F). These results suggest that when there is insufficient reduction in CV in G1, due to the inhibition of the G1/S transition, a compensatory reduction in CV emerges in S phase. Compensation also occurs when there is a greater reduction of CV in the G1 phase (under conditions when growth is inhibited by rapamycin) then there is less reduction of CV during the S phase.

Cell mass not only controls the duration of G1 but controls the duration of both the S and G2 phases.

To investigate cell size regulation outside of the G1 phase, we needed to optimize the resolution of the cell cycle markers that we employed. For that reason we adopted two cell cycle markers for live cells, mAG-hGeminin(34) and mTurquoise2-SLBP (35). The APC^{Cdh1} substrate geminin starts to accumulate in the nucleus at S phase entry(36), and the histone mRNA stem-loop binding protein SLBP is degraded rapidly at the very end of the S phase (37). With these two markers we could accurately quantify the duration of G1, S, and G2-M phases. Since the M phase duration is remarkably constant (14), we attributed most of the variation in G2-M duration to the G2 phase. We verified that the markers faithfully report the timing of the cell cycle phases and did not affect the length of cell cycle phases or the size-dependent regulation of cell cycle phase length (S1 Text, Chapter3).

Using ceQPM, we first confirmed the well-established cell size-dependent regulation of G1 length. Consistent with previous findings(3,4,6–8,11), we found that the G1 length was negatively correlated with birth mass in both transformed and non-transformed cell lines, HeLa and RPE-1, respectively (Fig. 2A, Fig. S4A). The correlation was stronger in RPE-1 than in HeLa cells (Fig. 2E, Table S3). We next investigated the mass-dependent regulation of the length of the S and G2 phases. In a previous study, Cadart et al. found a negative correlation between cell mass and the length of the nonG1 phases in HeLa cells, but did not distinguish the contributions of the S and G2 phases(7). In agreement with their finding, we discovered that both the S and G2-M phases are negatively correlated with the initial mass of the corresponding period in HeLa cells (Fig. 2B, C). Moreover, we found that the negative correlation was demonstrably stronger in S phase, than in G1 or G2-M (Fig. 2E, Table S3). We also found similar evidence for S and G2 regulation in RPE-1 cells. For RPE-1 cells, the correlation of S and G2-M phases with cell mass was weaker than in G1, yet in both cases the negative correlation was significant (Fig. 2E, Fig. S4B-C, Table S3). The results with RPE-1 cells implied that S and G2 regulation of cell mass can occur in a non-transformed cell with an intact cell cycle network including an intact G1/S transition. It is also worth noting that, although RPE-1 has tighter G1/S control than HeLa, the overall dependency of cell cycle length on cell mass was not stronger (Fig. 2D-E, Fig. S4D, Table S3). These analyses demonstrate that the size-dependent cell cycle regulation is not determined solely by the length of the G1 phase but rather also by changes in the lengths of the other phases of the cell cycle. To reinforce the importance of cell size control outside of the G1/S transition, we perturbed G1/S control in RPE-1 by 50 nM palbociclib,

which significantly prolonged the G1 length (Table S2) and increased the mean cell mass (Fig. 1G) as cells reached cell mass homeostasis. We found that the treatment of RPE-1 with palbociclib rendered the cell mass vs. cell cycle phase length correlations closer to those of HeLa cells. The size-dependent G1 regulation in the palbociclib treated RPE-1 cells was dramatically weaker; the G2 regulation was slightly weaker; notably the S regulation became the strongest among all the cell cycle phases (Fig. 2E, Fig. S4E-G, Table S3). Overall size-dependent cell cycle regulation was weaker than in untreated cells (Fig. 2E, Fig. S4H, Table S3). Collectively these results show that when much of the G1/S control is inactivated, as in HeLa cells, or in RPE-1 cells treated with palbociclib, S phase can compensate for weakened G1 length regulation and become the primary cell cycle phase of cell mass CV reduction (Fig. 1K, O).

Figure 2. The lengths of G1, S, and G2 phases are negatively regulated by cell mass. (A-D) The correlation between G1 (A), S (B), G2-M (C), and full cell cycle (D) length and the initial mass of the corresponding period in HeLa cells; each gray dot is an observation. Raw data are binned by cell mass, and each bin has the same cell number. Black squares indicate the average of each bin; error bars are the standard error of the mean (SEM). Solid red lines are the best fit of the black squares (Table S3). The red shaded area of the cell mass distribution in the top panels indicates the cell mass range that hits the minimal cell cycle phase length; the percentage is 100 minus the percentile of the fitted transition mass x_0. (E) Kendall's tau of the correlations between cell mass and cell cycle phase length in HeLa, RPE-1, and RPE-1 in 50 nM palbociclib or 100 nM rapamycin at cell mass homeostasis; the value and significance are summarized in Table S3. (F) The correlation between birth and division mass in HeLa cells. Each gray dot is an observation; black squares are the average of each cell mass bin, error bars are SEM. The solid black line is the best linear fit of the gray dots; the text indicates the function of the best fit. The red line is the prediction of the best fit in (D), assuming cells grow exponentially (Materials and Methods).

A closer look at the binned correlations reveals a fixed minimum limit to the length of a cell cycle phase, such that it will not shorten further even for very large cells (Fig. 2A-D, S4). Similar limits were found in the G1 phase in previous studies (3,7). To test the significance of the apparent limits, we fitted the binned correlations with two alternative models: Model 1, a linear model $y = a_1 x + b_1$ and Model 2, a piecewise model $y = a_2 x + b_2$ $(x \leq x_0)$, $y = a_2 x_0 + b_2$ $(x > x_0)$, where y is the cell cycle phase length, x is the initial mass, a_1, b_1, a_2, b_2, and x_0 are the fitting parameters. We used the Akaike Information Criterion (AIC) to compare the goodness of fits. A smaller AIC indicates a better fit, and the relative likelihood p_1 or p_2 predicts the probability that the alternative model is a better fit when Model 1 or 2 has the smaller AIC (38) (Table S3). We found that the piecewise model was a significantly better fit in all phases of HeLa cells, as well as the G1 and S phases in RPE-1 and S phase in RPE-1 with palbociclib. The linear model fit better in all other cases; this could be due to noise in the binned data. A significant limit implies that size-dependent cell cycle phase regulation fails to adequately control a substantial fraction of cells. Simulations indicate that the homeostatic birth size CV becomes much larger as the transition mass x_0 gets smaller, and the system eventually loses homeostasis when x_0 is smaller than the 40th percentile of the population (Fig. S5A, B). In addition, we found the slope between the birth and division masses is close to 1 in both HeLa and RPE-1, consistent with the adder-like behavior described previously (7). However, the fitted functions of birth mass and cell cycle length could not explain the adder behaviors, especially in large cells, assuming exponential growth (Fig. 2F, Fig. S4M-N). The

deviations are at least partially due to the minimal cell cycle phase length and imply that there is a necessity for a process of non-exponential growth (or growth rate modulation) to maintain cell mass homeostasis.

Previous studies suggested that there was a coordination of growth rate with cell cycle length(8,10). To investigate how growth rate affects cell cycle regulation, we inhibited growth by rapamycin, a specific mTOR inhibitor, in RPE-1 cells and measured cell cycle progression, after cells had reached cell mass homeostasis. Treatment with rapamycin lengthened the cell cycle (Table S2), and decreased cell mass (Fig. 1G); similar responses were previously observed (8,10). Under such conditions the control of G1 length became much stronger (Fig. 2E, Fig. S4I, Table S3), which is also consistent with previous findings(11), yet the control of the S and G2-M phases were virtually unchanged, except for a slightly extended S phase length (Fig. 2E, Fig. S4J-K, Table S3). The relative strength of the correlations between cell mass and cell cycle phase length in different phases coincides with the reduced CV in the corresponding phases, which demonstrates that inhibition of mTOR activity drives the largest reduction in the cell mass CV to occur in the G1 phase (Fig. 1P). Furthermore, the negative correlation between birth mass and cell cycle length was stronger in rapamycin than in untreated cells or palbociclib treated cells (Fig. E, Fig. S4L, and Table S3). Cell cycle length as a function of birth mass in rapamycin also fits the birth mass vs. division mass correlation better under the assumption of exponential growth (Fig. S4O). The result suggests that rapamycin suppresses growth rate modulation, and when growth rate modulation is suppressed, cell cycle regulation predominates in cell mass homeostasis.

Size-dependent growth rate modulation can generate significant reductions in CV during the cell cycle and is comprised of both mTORC1 dependent and independent components.

A simple view of cell growth kinetics, absent any mass sensing and feedback, should be exponential due to the autocatalytic nature of mass dependent growth, which is particularly clear for ribosome dependent ribosome biosynthesis. However, several studies have found that although large cells generally grow faster than small cells, growth is not exactly exponential (7,28,39). Generally, dependency of growth rate on cell mass changes with cell mass and cell cycle stages(7,8,19,27,40–42). Recent studies by us and others even demonstrated growth rate oscillations(28,43), where a cell alternates between increases and decreases in growth rate. To explore the dependence of growth rate on cell mass in proliferating cells, we measured the growth rate in a 3-hour time window and investigated its correlation with cell mass at 0 hours. We verified that the observed cell mass vs. growth rate correlations in the short-term measurements were consistent with the long-term growth trajectories and genuinely reflected growth modulation during the cell cycle (S1 Text, Chapter6). In agreement with previous findings, the mass vs. growth correlation in HeLa cells was close to exponential, except for a slight deviation for large cells (Fig. S6A)(7,28). However, when segregating the cells into four cell cycle phases, the correlations displayed distinct cell cycle dependency, which was originally masked by pooling the cells (Fig. S6B). An even closer look revealed a positive-to-negative correlation transition at certain cell cycle stages (Fig. S6C). The slope of the linear relation between cell mass and growth rate indicated stronger modulation in the late G1 and G2-M phases, consistent with Fig. S6B and previous studies (8,33). However, the proportionality is lower than exponential in most of the cell cycle stages (Fig. S6D), suggesting a global mechanism that limits the growth of large cells in addition to cell cycle-specific regulatory features. Investigating the mass vs. growth correlations in finely divided cell cycle stages reveals subtle features. Yet such studies require large numbers of cells and very accurate cell growth rate measurements. Coarser cell cycle discrimination leads to some loss of information on subtle

changes in the growth rate but adds greater statistical weight to conclusions about grosser features of size-dependent growth regulation. Therefore, in the following analyses, we made a binary partition of cells into the G1 and nonG1 phases, and focused on the most vivid features of growth rate modulation.

When we measured the correlation of cell mass with growth rate in five cell lines, we found that no two cell lines behaved the same. In Saos2 cells, growth was exponential except for a slight deviation for large cells in the nonG1 phases (Fig. S7A). In HeLa cells, the growth in large cells was slower than exponential in both G1 and nonG1 phases (Fig. 3A). In RPE-1 cells, growth was proportional to cell mass, but the proportionality was much less than exponential with a significant nonzero intercept (Fig. 3B). In HT1080 cells, the growth was close to exponential in small cells but transited to almost linear in large cells in both G1 and nonG1 phases (Fig. 3C). In U2OS cells, the correlation was close to exponential for all cells in nonG1 and most cells in G1 phase but was abruptly negative in the 15% largest cells in G1 phase (Fig. S7B). To test whether the transitions we saw in the growth rate vs. mass curves were significant, we used two alternative models to fit the binned correlations: a linear model $y = ax + b$ and a piecewise model $y = cx + d\ (x \leq x_0), y = ex_0 + f\ (x > x_0)$, where y is the growth rate, x is the cell mass, a, b, c, d, e, f, and x_0 are the fitting parameters. As introduced in the preceding section, we used the Akaike information criterion (AIC) to estimate the goodnesses of fits. The piecewise model was significantly better in the nonG1 phase in SoaS2 and HT1080 cells (Table S4). Strikingly, when U2OS cells were cultured in DMEM with 10% FBS, a suboptimal medium with limited nutrients, the transition to negative correlation in the G1 phase became significant, and the transition mass x_0 was smaller (Fig. 3D, Table S4). As the apparent correlation was a combination of cell cycle and cell mass dependencies, the change could be attributed either to the modulation acting on smaller cells or starting earlier in the cell cycle or both. Similarly, low serum medium converted the mass vs. growth correlation from positive to negative in the G1 phase in RPE-1 cells (Fig. S7C). The results in U2OS and RPE-1 suggest that limited nutrients or low serum strengthens growth rate modulation in the G1 phase.

Figure 3 Growth rate modulation is in different forms in different cell lines and composed of mTORC1-dependent and mTORC1-independent processes. (A-D) Correlations between cell mass and growth rate in the G1 (red) and nonG1 phases in different cell lines. Filled squares are the median growth rate of each bin; error bars show SEM. Black dashed lines indicate exponential growth. Solid blue and red lines are the best fit of the filled squares (Table S4). (E) The correlation between cell mass and phosphorylated RPS6 as the mTORC1 activity reporter in U2OS cells in DMEM. Solid lines are the best fit of the filled squares (Table S5). (F-H) Correlations between cell mass and growth rate in U2OS cells in 100 nM rapamycin (F), 100 nM cycloheximide (G), and 10 µM MG132 (H) right after adding the drugs. Solid green and orange lines are the fitted correlations of untreated cells. (I) mTORC1-dependent and mTORC1-independent growth together constitute the observed cell mass vs. growth rate correlation. (J) Model of growth rate modulation: mTORC1-dependent and mTORC1-independent growth are regulated separately; they can form positive or negative feedback loops with cell mass. Rapamycin weakens the mTORC1-dependent loop by inhibiting mTORC1 activity.

We found two general types of growth rate modulation. In the first, growth is linearly related to cell mass, but with a slope lower than exponential (Fig. 3A, B, Fig. S7C, Table S4). In the second, the correlation between cell mass and growth rate consists of exponential growth for small cells but is less positive or even negatively correlated in large cells (Fig. 3C, D, Fig. S7A, B, Table S4). To investigate the implications of growth rate modulations on the cell mass CV, we simulated the results by a model where we assumed that all cells divide at the same cell cycle length. When cells grow exponentially, the cell mass CV increases super-exponentially due to the variability in growth rate (S1 Text Chapter5, Fig. S8 B, D). As the slope of the correlation of growth rate with cell mass decreases, the more the cell mass CV is reduced during the cell cycle (Fig. S8). We found that a moderate deviation from exponential growth (in all cells or in just large cells) is itself sufficient to maintain the birth mass CV at homeostasis without any need to regulate the cell cycle (Fig. S8). These models, inspired by the data itself, gave us the hint that in many cases a small deviation from exponential growth was sufficient in itself to make significant impact on cell mass CV reduction and maintain cell mass homeostasis. We explore below how such a process may be implemented in different cell lines.

Although the manner and extent of cell growth rate modulation differ in different cell lines, it seemed unlikely that each cell line would employ a unique growth control mechanism. We therefore looked for some universal regulatory strategy that might explain the diverse cell mass vs. growth rate correlations that we observed. We focused on growth modulation in U2OS cells in suboptimal medium (DMEM), which had the striking feature of a regime where there is a negative slope of growth rate with mass imposed early in the cell cycle. As mTORC1 is the major signaling pathway that senses nutrients and growth factors, we investigated whether it was involved in this process(44). We used phosphorylated RPS6 (p-RPS6), a downstream substrate of the mTORC1 pathway, to report its activity(45,46) on the individual cell level. We found a positive correlation between p-RPS6 and growth rate in both the G1 and nonG1 phases (Fig. S9C). However, in DMEM, p-RPS6 of U2OS cells was heterogeneous in level and displayed a bimodule distribution (Fig. S9A, B). In the nonG1 phase, p-RPS6 was positively correlated with cell mass (Fig. 3E). The correlation changed abruptly from positive in small cells to negative in large cells within the G1 phase (Fig. 3E). This transition of p-RPS6 vs. cell mass correlation and the point in the cell mass spectrum where the transition occurred, coincided with the change in the slope of cell mass vs. growth rate correlation (Fig. 3D). This was a striking coincidence, suggesting that the negative correlation between cell mass and growth rate in U2OS is likely caused by the mTORC1 activity. We, therefore, examined the effects of inhibiting mTORC1 by rapamycin. It is worth noting that rapamycin acutely inhibits mTORC1 whereas chronic exposure also inhibits mTORC2(47). However, neither the short-term nor long-term rapamycin treatement inhibited growth entirely. When mTORC1 activity was completely suppressed at the saturated concentration of rapamycin (Fig. S9D), the growth rate was reduced less than 25% (Fig. S9E). Remarkably, the negative correlation between cell mass and growth rate was absent in saturated rapamycin, revealing a residual propensity for exponential growth (Fig. 3F). Similar behaviors were seen in RPE-1 cells, where super-linear growth became much closer to exponential in rapamycin (Fig. S9F), suggesting to us that cell growth is comprised of both an mTORC1-dependent and an mTORC1-independent component. Size-dependent growth modulation in the G1 phase in U2OS is mainly determined by the mTORC1-dependent part, whereas the mTORC1-independent growth becomes essentially exponential and is unaffected by rapamycin. As we could not directly measure the mTORC1-dependent growth, we assumed its correlation with cell mass was similar to p-RPS6 (Fig. 3I). The sum of the two components constitutes the observed cell mass vs. growth correlation (Fig. 3I). Since cell growth is the net sum of protein synthesis and degradation(48) and

mTORC1 regulates both (49,50), we further investigated whether growth rate modulation is due to protein synthesis or protein degradation or both. When protein synthesis was moderately inhibited by the translation inhibitor cycloheximide(51), the global growth slowed down, the mass vs. growth correlation in large cells was less negative, but the transition in the correlation of growth with size from positive to negative was still just shy of significant at a similar transition mass compared to control (Fig. 3G, Table S4). However, when protein degradation was inhibited by the proteasome inhibitor MG132(52), the global growth rate was slightly faster and very close to exponential (Fig. 3H). These results suggest that the growth rate modulation in the G1 phase is mainly mediated through protein degradation, not protein synthesis, consistent with indirect hints in previous studies(33,41). We therefore conclude that the negative correlation between cell mass and growth rate in U2OS is mediated by mTORC1, principally through the regulation of protein degradation.

We also investigated the near-linear growth in RPE-1 cells in a low concentration of palbociclib (Fig. S10A). It is similar to what has been observed in excessively large cells generated by cell cycle arrest in previous studies(7,19). It was first proposed that a linear growth versus mass curve was a result of DNA limitation, when replication was inhibited and/or due to effects of cytoplasmic dilution on cell growth(19,53). However, as shown in Fig. S10B, mTORC1 activity (and mTORC1-dependent growth) was positively correlated with cell mass in cells treated with palbociclib. By contrast, mTORC1-independent growth revealed by rapamycin was negatively correlated with cell mass in those cells (Fig. S10C). It seems likely that there is no mechanism that directly causes the linear growth behevior; rather it can be explained most easily as a composite of positive (mTORC1-dependent) and negative (mTORC1-independent) processes (Fig. S10D). As expected, cycloheximide decreased and MG132 slightly increased the average growth rate, but neither caused a significant change in the slope of the growth versus mass correlation in palbociclib treated cells (Fig. S10E, F), suggesting that the growth regulation in excessively large cells generated by cell cycle arrest is different from the mechanisms utilized in limited nutrient or serum conditions. The cause of the negative correlation between mTORC1-independent growth and cell mass in excessively large cells is still mysterious and will require futher investigation.

In summary, we propose a model of growth rate modulation, where growth is comprised of mTORC1-dependent and mTOC1-independent components. Each component is regulated separately and can form a positive or negative feedback loop with cell mass through unknown size-sensing mechanisms. We speculate that the combination of the two components produces various forms of growth modulation, seen in different cell types or in the same cell type under different growth conditions or pharmacologic perturbations.

Other possible explanations for the cell mass CV reduction in the cell cycle

We investigated other potential processes that could explain the observed cell mass CV reduction. In principle, any process that differentially affects the probability of cell division or viability in large and small cells would influence the cell mass distribution in the population. Therefore, we investigated the rate of cell death and cell cycle arrest in long-term cell growth and proliferation measurements. During the 48 or 72 hours that we measured cells, we identified cell cycle arrest events as having occurred when a cell stayed at the same cell cycle phase, while the cell mass kept increasing throughout the duration of the experiment. Whereas cell death was identified by the collapse of the cell body. We found that the cell cycle arrest and cell death events were rare (no more than 2%) in all the cases we investigated (Table S5), meaning that neither cell cycle arrest nor cell death is very likely to contribute

significantly to the mechanism of cell mass homeostasis in these experiments. Note that the extremely low frequencies of cell cycle arrest in rapamycin and palbociclib suggested that very few cells were arrested in quiescence or senescence at the drug concentrations used in this study, which is consistent with the fact that rapamycin only moderately reduced the cell growth rate at less than 25% (Fig. S9E) and palbociclib at the concentration used in this study only extended the cell cycle length by 33% (Table S2). We also discovered that large RPE-1 cells in palbociclib had a higher probability of losing a portion of cytoplasm during mitosis (Table S5, Movie S1), which has not been previously reported to the best of our knowledge. The cytoplasmic loss may be due to incomplete cortical contraction during mitotic rounding(54) and the lost mass seems to be random. But again, the events were much too rare (about 0.5% in the population) to be of significance in maintaining cell mass homeostasis.

Cell mass homeostasis in proliferating cells is the result of multiple control processes.

Homeostasis is a balance between noise in cellular processes and feedback control. In proliferating cells, noise comes from stochasticity in growth rate, cell cycle length, and cell mass partition at mitosis. Cell mass variation can be reduced by size-dependent regulation of either the progression through the cell cycle or growth rate or both. To evaluate the factors that could play significant roles in maintaining cell mass homeostasis under realistic conditions, we built a stochastic model to simulate the growth of a cell population and fed in parameters extracted from the experimental data (S1 Text, Chapter7). Although it is simplified, the result qualitatively reflects the impact of those features that we found to be important. We evaluated this model for HeLa and RPE-1 cells, as well as RPE-1 in rapamycin and palbociclib. We considered three factors that might increase cell mass variation: variability in cell cycle length, variability in growth rate, and asymmetry in mitotic division. We found that the largest contributor to cell mass variation in a population for all four cases (Fig. S11A-D) was the variability in growth rate. The asymmetry of the mitotic division also has considerable influence, as it directly affects the birth mass CV of the next generation (Fig. S11 A-D). The impact of cell cycle variability is relatively small (Fig. S11 A-D). Three major mechanisms oppose these factors and cause the CV reduction in cell mass. They are: G1 length control, nonG1 length control and growth rate modulation. Given that nearly all of the attention for explaining cell mass homeostasis has been on G1/S timing (1,18), it surprised us that G1 length regulation, when measured carefully in two cell types, did not make the largest contribution. Specifically, G1 length regulation played only a slightly larger role than the nonG1 regulation and much smaller role than the growth rate modulation in RPE-1 cells with intact G1/S control (Fig. S11B). This might be in part due to the relatively short duration of the G1 phase in RPE-1 cells, which is about two-thirds of the nonG1 phases (Table S2). However, G1 length regulation only becomes a major control mechanism when the growth modulation is inhibited (by rapamycin) (Fig. S11C). When the G1/S control is inhibited by palbociclib or mutated as in HeLa cells, the nonG1 length regulation and the growth rate modulation become even more dominant (Fig. S11A, D). In particular, growth rate modulation plays its most critical role in cell mass CV reduction in both HeLa and RPE-1 cells (Fig. S11 A, B). This is particularly surprising, as we note that growth only slightly deviates from exponential in large HeLa cells (Fig. 3A). This finding, by itself is a strong indication that a form of growth control where there is a moderate deviation from exponential growth effectively reduces cell mass CV, as illustrated by the simulation in Fig. S8.

To visualize size regulation as a balance of sources of noise and sources of compensatory mechanisms, we have drawn a “teeter-totter” representation of cell mass homeostasis (Fig. 4). The stochastic noise and the control mechanisms are analogous to weights on the left and right sides of the lever’s fulcrum,

respectively. They balance when the system is steady state. In wild-type cells like RPE-1, the relative weight of the control mechanisms, from heaviest to lightest are: growth rate modulation, G1 length regulation, and nonG1 length regulation. When G1/S control is inhibited by drug or genetic mutation, the G1 length regulation contribution is reduced (i.e. weighs less), and the nonG1 length regulation and growth rate modulation contribute more and retain the balance. When growth rate modulation is inhibited by suppressing mTORC1 activity, the G1 length regulation weight becomes heavier. Overall, the cell mass homeostasis teeter-totter is robustly balanced by the compensations of different control mechanisms.

Figure 4 The teeter-totter model of cell mass homeostasis abstracted from Fig. S11. Cell mass homeostasis requires balanced stochastic noise and control mechanisms. In non-transformed cells, the weights of control mechanisms from the heaviest to the lightest are the growth rate modulation, G1 length regulation, and nonG1 length regulation. When the G1/S control is perturbed, the impact of the G1 length regulation becomes smaller, and the nonG1 length regulation and growth rate modulation become larger. When the growth rate modulation is suppressed by inhibiting mTORC1 activity, the G1 length regulation plays a more prominent role in compensating.

Discussion

In our study of cell mass homeostasis, we found that stochastic variation in cell mass in proliferating cells is tightly controlled throughout the cell cycle via size-dependent modulation of cell growth and size-dependent regulation of cell cycle progression (Fig. 1-3). The compensation that keeps stochastic variation of size in check emerges from an interplay of multiple mechanisms and results in cell mass homeostasis. Not only is homeostasis maintained, but it is also maintained at high stringency, as indicated by the narrow distribution of cell birth mass. In many circumstances where this has been observed, it seems very robust against changes in genetic background resistant to manipulations of the G1/S transition or mTORC1 perturbation (Fig. 1). In many bacterial, yeast, mammalian, and plant cells, the birth mass CV also falls in a relatively small range (from 11% to 25%) (Table S7), comparable to the birth weight CV of a human fetus(55). Although it is not clear whether such strict control is intentionally optimized during evolution or merely a by-product of some other selection (56), cell mass homeostasis appears to be highly regulated and likely to be important. Though we focused on cultured human cell lines in this study, the mechanisms underlying cell size homeostasis, just as the mechanisms underlying the cell cycle, are likely to be conserved in cell types in vivo and in many species.

In this study we systematically investigated factors that affect cell mass variation. Benefitting from the accuracy and high throughput of ceQPM(28), we were able to accumulate sufficient data to derive meaningful correlations between cell mass and cell cycle and between cell mass and growth rate and fit such data by simple functions (Fig. 2-3). We could show how G1, S, and G2 phases are each under negative regulation by cell mass in both transformed and non-transformed cell lines (Fig. 2). We offer a plausible explanation of why cell cycle regulation has a limited impact on large cells, in terms of a minimum length for each cell cycle phase. Simply put, a phase of the cell cycle cannot shorten enough below its minimum length to compensate for cells of very large size (Fig. 2). We demonstrated that growth rate is modulated in different ways in different cell types or cell lines (Fig. 3). This basic

characterization of growth regulation was not previously possible without the extensive and precise measurements of cell mass and growth rate by ceQPM. These results encouraged us to further analyze cell growth, leading to a picture of mass growth in cells, which is composed of separately regulated mTORC1-dependent and mTORC1 –independent processes. We could further show by ceQPM that the cell mass distribution of the proliferating population was not significantly affected by cell death, cell cycle arrest, or cytoplasmic mass loss at mitosis (Table S6). Although these are of negligible importance in the experimental setting, such mechanisms might play a more significant role in a tissue setting, for example during wound healing, regeneration and aging.

Although it has been widely assumed that the G1 length regulation is the predominant (or the only) mechanism controlling cell size during the cell cycle, we found that the impact of G1 length regulation on reduction of the CV of a population of growing cells is significantly less than the impact of growth rate modulation. This is true even in non-transformed cells with intact G1/S control (Fig. 4, Fig. S11). The contribution of G1 length control only becomes significant when growth rate modulation is inhibited. Under conditions where G1/S control is perturbed, as for example by palbociclib in RPE cells or in HeLa cells, S phase regulation and growth rate modulation together compensate for the lost function of G1 length control and maintain the birth mass CV at the same level (Fig. 1, 4). Why have more than one mechanisms of size control? We propose that the G1/S regulation may play a critical role in the process of *setting* cell size but not in the process of *maintaining* cell size homeostasis. Rather, the maintenance of homeostasis occurs through circuits of multiple processes compensating for each other. It would make more sense that the targeted *mean* size is controlled by a few key molecular players downstream of specific hormonal or nutrient signals, changes in environmental conditions or cellular differentiation. Those molecular players (such as CDK4) were known as cell size "dial" in a previous model by Tan et al.(10). However, after cells are programmed to adopt a defined size in their new state, they would still require mechanisms to maintain size homeostasis around that new mean. Consistent with our work (Fig. 1) and studies in budding and fission yeasts(12,16), deletion or overexpression of the G1/S inhibitors changes the mean size dramatically but has only small effects on cell size variation. Furthermore, systems that deploy multiple mechanisms, continuously monitoring and adjusting size variation, may have a clear advantage over a system that only provides a gate for size variation at a specific cell cycle checkpoint(57). However, that gate, which can act at only one point of the cell cycle, and an early one at that, would not be able to provide continuous feedback with cell size throughout the cell cycle (Fig. 3, Fig. S8). This distinction seems to be the case for all the cells we examined, where cell mass is regulated, and the CV is reduced significantly throughout the cell cycle (Fig. 1).

There is still a missing ingredient to this model of cell size homeostasis. Modulating the time in G1 through regulation of the G1/S transition as a function of mass provided a simple model of how cell size could affect the mass accumulation in G1, the length of the cell cycle, and hence the size distribution. However, for cell size to be controlled throughout the cell cycle in response to the rate of mass accumulation would require a mechanism, whereby a cell constantly knows how large it is and can respond by regulating its protein levels accordingly. But how do cells sense their size? It is worth noting that, to maintain size homeostasis, cells only need to sense their relative size compared to the mean without knowing the targeted size. The fundamental principle of cell size sensing relies on some form of disproportionality of molecular components or signals to size. For instance, cells sense size through the sub-scaling of inhibitors or super-scaling of activators to regulate their cell cycle length(9,58). Cell mass accumulation requires coordinated transcription, translation, nutrient uptake, and ATP generation(53).

Each process feedbacks to others and may increase with cell size at a different rate. Any break of the coordination might serve as a size sensor. It has been proposed that cells may sense size and modulate growth rate by DNA limitation, cytoplasmic dilution, surface-to-volume ratio, sublinear proportionality between metabolic rate and cell mass, transportation efficiency, and other mechanisms(19,53,57,59,60). We found that growth rate modulation is composed of separately regulated mTORC1-dependent and mTORC1–independent processes, which may sense size through different mechanisms. It has been proposed that p38 MAPK may sense size and activate mTOR during development(11). Since mTORC1 senses nutrients(61,62), and its modulation on cell growth rate is likely through protein degradation (Fig. 3), we wondered whether size sensing could be related to the amino acid pool size, which reflects the flux of nutrient intake, protein synthesis, and destruction. We are still rather ignorant of in how the mTOR pathway integrates the upstream signals through a complex network of many kinases and determines downstream global responses, eventually modulating cell growth and through that, cell mass. It is probably not that simple. Besides cell mass-dependent modulation, growth rate is also regulated in a cell cycle-specific manner and oscillates intrinsically(28,40,42,43). The coexistence of multiple forms of regulation complicates any investigation. It would be helpful to isolate each mechanism for study, by searching for conditions where only one of the processes is dominant.

Aside from the regulation on G1 length and general growth rate, the regulation on S and G2 length also contributes to the cell mass CV reduction, especially when the G1/S control is compromised. The mechanism of G2 length regulation has been mainly studied in fission yeast, where the G2/M transition acts as the major size control checkpoint(16,63–65). Mammalian and fission yeast share homologous components of their G2/M regulation(66,67); thus the mechanisms working in fission yeast for cell size control might also function in mammalian cells, although there has not been any evidence for that. Regulation on S phase length, as a means for control of cell mass in mammalian cells, has been rarely explored. One possible mechanism of the S phase regulation is that the number of replication complexes might be proportional to the total cell mass, and small cells might make fewer folks, which could limit the rate of S phase progression (68). If cell mass were to affect the number of active origins or DNA replication speed, it might also affect the level of DNA damage due to the under- or over-replicated regions(68–70). Thus tumorigenesis or senescence might take place preferably in large or small cells. This condition may be very common, as more than 20% of non-transformed cells carry DNA lesions in the G1 phase, indicating that there is replication stress in a normal cycling population(71). Nonetheless, it is worth noting that cells hit the minimal S phase length at a larger cell mass and the negative correlation between cell mass and S phase length becomes stronger in palbociclib than untreated RPE-1 cells, suggesting more complex crosstalk between the G1 and S phase regulations than such a simple explanation.

There have been several phenomenological models for cell size control that have been applied to bacterial and mammalian cells. In 2015, Taheri-Araghi et al. found that E. coli cells behave as an “adder”, where a constant volume is added during each cell cycle(72). It is believed that in E. coli and other bacteria, the adder behavior is governed by DNA replication and division proteins(73,74). Later, measurements of cell size in budding yeast and many mammalian cell lines also found that they behaved phenomenologically as an adder (7,75,76). While this seemed to have offered a powerful generality in cell size control, spanning bacteria and eukaryotes, the cell cycle processes in budding yeast and mammalian cells are very different from bacteria. This similarity has not led to the discovery in budding yeast or mammalian cells any process that explained the phenomenological adder behavior(14,77).

Instead, Chandler-Brown et al. proposed that there is no mechanistic adder molecule in budding yeast, and the observed adder is the combination of a G1 "sizer" and a nonG1 "timer"(78). In this view, the adder is not a mechanism per se, but more likely a fortuitous quantitative coincidence of the simple adder model and the complex quantitative growth dynamics. It was also believed to be the case in mammalian cells: the G1/S regulation of size forms a "sizer" in G1 phase, and the uncontrolled nonG1 phase behaves as a "timer"(18). The problem of this explanation, as already discussed, is that mammalian cell size is not simply regulated by coupling cell division to the attainment of a specified size in G1. The nonG1 phases participate in cell size control and often outweigh the G1 length control. Furthermore there does not appear to be a constant interval where cells grow exponentially. There is also no evidence for an "adder" protein or pathway in mammalian cells that senses the accumulated mass throughout the cell cycle and constantly adjust it. Using our more accurate mass measurements, we have confirmed the adder "behavior" in HeLa and RPE-1 cells (Fig. 2F, Fig. S5M); RPE-1 cells in palbociclib or rapamycin also behave as an imperfect adder (Fig. S5P, O). When evaluating the cell cycle phases individually, untreated RPE-1 cells or cells exposed to rapamycin support the non-mechanistic adder model over the whole cell cycle: the added masses of the neighboring phases do not correlate (Fig. S12A-J). This means that the neighboring phases are independently regulated by size, and there is no global "adder" that governs the whole cell cycle. Note that in rapamycin, the correlation between added masses of neighboring phases of the cell cycle are closer to zero than in untreated cells, suggesting that the neighboring cell cycle phases are even more insulated in growth rate inhibition. However, when the G1/S control is inhibited (in HeLa and in RPE-1 treated by palbociclib), the correlation between the added masses of neighboring phases becomes much more significant (Fig. S12K-T), suggesting the existence of some compensation among the cell cycle phases and this might suggest an "adder" mechanism continuously sensing of the added mass throughout the cell cycle. Since growth rate modulation plays a more significant role in those cases, we wonder focusing on growth rate modulation may ultimately lead to a better understanding of the "adder-like" behavior of mammalian cells.

The use of ceQPM to quantify single-cell dry mass, mass growth rate, and cell cycle progression has provided the most accurate, complete, and quantitative description of cell mass homeostasis in mammalian cells. Size (mass) dependent growth throughout the cell cycle appears to be the dominant feature of cell size control. Further study of this mechanism promises to lead us to a molecular understanding of size homeostasis. Understanding the mechanism of cell size regulation in proliferating cells may also lead us to an understanding of size homeostasis in non-dividing cells, the cell state of most adult human tissues. G1 length control, which makes some contribution to size homeostasis, may in the end be most related to establishing the size of a cell in the differentiated state and could also be very important in embryogenesis and regeneration. It appears that we are still at an early stage of defining the phenomenon of size homeostasis and still far from understanding the regulatory circuits that tell a cell how large it is at a given cell cycle state. How this feeds back on the anabolic or proteostatic machinery is central and still unanswered question.

Materials and Methods

Cell Culture and Chemical Treatment. HeLa mAG-hGem, RPE-1 mAG-hGem, HT1080 mAG-hGem mKO2-hCdt1, and HeLa mAG-hGEM DNA-ligase-dsRed cells were made in previous studies by our laboratory(33,46). U2OS mAG-hGem and SaoS2 mAG-hGEM cells were generated by lentivirus infection. Lentivirus carrying mTurquoise2-SLBP was purchased from Addgene (83842-LV) to make HeLa mAG-hGem mTurquoise2-SLBP, RPE-1 mAG-hGem mTurquoise2-SLBP, and HeLa mAG-hGEM DNA-ligase-

dsRed mTurquoise2-SLBP. Single clones of stable expression were selected for each cell line. Cells were incubated at 37 °C with 5% CO2 in Dulbecco's modified Eagle's medium (DMEM) (11965; Thermo Fisher Scientific) with 25 mM Hepes (15630080; Thermo Fisher Scientific) and 10 mM sodium pyruvate (11360070; Thermo Fisher Scientific) or McCoy's 5A medium (16600082; Thermo Fisher Scientific). Both media were supplemented with 10% fetal bovine serum (FBS) (16000044; Thermo Fisher Scientific) and 1% penicillin/streptomycin (15140122; Thermo Fisher Scientific). Palbociclib and MG132 were purchased from selleckchem (PD-0332991 and S2619), rapamycin was purchased from LC Laboratories (R-5000), and cycloheximide was purchased from Millipore Sigma (C4859).

Live Cell Imaging. Cells were imaged at 10X magnification by an Eclipse Ti microscope with the Perfect Focus System (PFS) (Nikon, Japan) and SID4BIO camera (Phasics, France). NIS-Elements AR ver. 4.13.0.1 software with the WellPlate plugin was used to acquire images. A home-made incubation chamber was used to maintain a constant environment of 36 °C and 5% CO2. Cells were seeded on 6 well glass bottom plates (P06G-1.5-14-F; MatTek) at a density of 1500 cells/cm^2 3 h before long-term imaging or 3500 cells/cm^2 16 h before short-term imaging. Before the time lapse started, mineral oil (M8410; Millipore Sigma) was added into each well to prevent evaporation. In the long-term experiments studying the cell cycle regulation, cells were monitored for 48 or 72 h. In the short-term experiments studying growth rate modulation, cells were monitored for 3 h. For all experiments, the phase images were acquired every 30 min, and the fluorescent images were acquired every 1 h.

Fixation and Immunostaining. After the short-term time-lapse, the mineral oil was gently removed by aspiration. Cells were fixed with 4% paraformaldehyde (RT 157-8; Electron Microscopy Sciences) and stained with Hoechst 33342 at 1 µM (62249; Thermo Fisher Scientific). The cells were imaged by QPM again to identify their cell cycle stages. To detect the activity of mTORC1, fixed cells were treated with the blocking buffer (2% BSA + 0.3 M glycine + 0.1% Tween 20 in PBS) for 1 h, then incubated with the primary antibody of anti p-RPS6 rabbit mAb (1:100, 4858; cell signaling technology) at 4 °C overnight. After incubated with the secondary antibody of goat anti-rabbit IgG (H+L) Alexa Fluor 568 (1:1,000, A-11011; Thermo Fisher Scientific), cells were stained with 250 ng/mL Alexa Fluor 647 NHS ester (A20006; Thermo Fisher Scientific) and 2 µM DAPI (4, 6- diamidino-2-phenylindole) (D8417; Sigma-Aldrich) and then imaged by the QPM and ORCA-ER (Hamamatsu, Japan) cameras on the same microscope. The fluorescent images from the ORCA-ER camera were registered to the QPM images of live cells mediated through the QPM image of fixed cells.

QPM Image Processing and Data Analysis. The QPM images were processed by the ceQPM method developed previously(28) and conducted on the O2 high performance compute cluster. To evaluate whether the cell cycle control could explain the adder behavior, we assumed cells grew exponentially at the rate of $\alpha = \ln(2)\,/DT$, where DT is the averaged cell cycle length. The division mass could be predicted by $m_d = m_b e^{\alpha T}, T = fun(m_b)$, where fun is the best fitted function in the alternative models of cell cycle length vs. birth mass.

Data Availability. Cell lines are available upon request. All data are included in the manuscript and supporting source data files.

Acknowledgements

We thank the National Institute of General Medical Sciences (5RO1GM26875-42) and National Institute on Aging (1R56AG073341-01) for grant support. We thank the Nikon Imaging Center at Harvard Medical School for providing space and sharing other resources. We thank the Research Computing Group at

Harvard Medical School for providing support for the O2 Compute Cluster for imaging processing and data storage. We thank Johan Paulsson, Ariel Amir, Prathitha Kar, Ethan Levien, Ahmed Rattani, Wenzhe Ma, Gabriel Neurohr, Simon Gemble, and Renata Basto for insightful suggestions. We thank William Ratzan for proof-reading the manuscript.

References

1. Ginzberg MB, Kafri R, Kirschner M. On being the right (cell) size. Science [Internet]. 2015;348(6236):1245075–1245075. Available from: http://www.sciencemag.org/cgi/doi/10.1126/science.1245075

2. Killander D, Zetterberg a. A quantitative cytochemical investigation of the relationship between cell mass and initiation of DNA synthesis in mouse fibroblasts in vitro. Exp Cell Res [Internet]. 1965 Oct;40(1):12–20. Available from: http://www.ncbi.nlm.nih.gov/pubmed/5838935

3. Varsano G, Wang Y, Wu M, Varsano G, Wang Y, Wu M. Probing Mammalian Cell Size Homeostasis by Channel-Assisted Cell Reshaping. CellReports [Internet]. 2017;20(2):397–410. Available from: http://dx.doi.org/10.1016/j.celrep.2017.06.057

4. Xie S, Skotheim JM. A G1 Sizer Coordinates Growth and Division in the Mouse Epidermis. Curr Biol [Internet]. 2020;30(5):916-924.e2. Available from: https://doi.org/10.1016/j.cub.2019.12.062

5. Dolznig H, Grebien F, Sauer T, Beug H, Müllner EW. Evidence for a size-sensing mechanism in animal cells. Nat Cell Biol [Internet]. 2004 Sep [cited 2012 Dec 5];6(9):899–905. Available from: http://www.ncbi.nlm.nih.gov/pubmed/15322555

6. Zatulovskiy E, Zhang S, Berenson DF, Topacio BR, Skotheim JM. Cell growth dilutes the cell cycle inhibitor Rb to trigger cell division. Science (80-) [Internet]. 2020;369(6502):466–71. Available from: http://science.sciencemag.org/

7. Cadart C, Monnier S, Grilli J, Sáez PJ, Srivastava N, Attia R, et al. Size control in mammalian cells involves modulation of both growth rate and cell cycle duration. Nat Commun [Internet]. 2018;9(1). Available from: http://dx.doi.org/10.1038/s41467-018-05393-0

8. Ginzberg MB, Chang N, Kafri R, Kirschner MW. Cell size sensing in animal cells coordinates anabolic growth rates and cell cycle progression to maintain cell size uniformity. Elife [Internet]. 2018;(1):123851+. Available from: http://dx.doi.org/10.1101/123851

9. Lanz MC, Zatulovskiy E, Swaffer MP, Zhang L, You DS, Marinov G, et al. Increasing cell size remodels the proteome and promotes senescence. bioRxiv. 2021;1–50.

10. Tan C, Ginzberg MB, Webster R, Iyengar S, Liu S, Papadopoli D, et al. Cell size homeostasis is maintained by CDK4-dependent activation of p38 MAPK. Dev Cell [Internet]. 2021 May;1–14. Available from: https://doi.org/10.1016/j.devcel.2021.04.030

11. Liu S, Ginzberg MB, Patel N, Hild M, Leung B, Li Z, et al. Size uniformity of animal cells is actively maintained by a p38 MAPK-dependent regulation of G1-length. Elife [Internet]. 2018 Mar 29;7(April):1–27. Available from: https://elifesciences.org/articles/26947

12. Chen Y, Zhao G, Zahumensky J, Honey S, Futcher B. Differential Scaling of Gene Expression with Cell Size May Explain Size Control in Budding Yeast. Mol Cell [Internet]. 2020;78(2):359-370.e6. Available from: https://doi.org/10.1016/j.molcel.2020.03.012

13. Zetterberg A, Larsson O. Kinetic analysis of regulatory events in G1 leading to proliferation or quiescence of Swiss 3T3 cells. Proc Natl Acad Sci U S A [Internet]. 1985 Aug 1;82(16):5365–9. Available from: http://www.pubmedcentral.nih.gov/articlerender.fcgi?artid=390569&tool=pmcentrez&rendertype=abstract

14. Araujo AR, Gelens L, Sheriff RSM, Santos SDM. Positive Feedback Keeps Duration of Mitosis Temporally Insulated from Upstream Cell-Cycle Events. Mol Cell [Internet]. 2016;64(2):362–75. Available from: http://dx.doi.org/10.1016/j.molcel.2016.09.018

15. Garmendia-torres C, Tassy O, Matifas A. Multiple inputs ensure yeast cell size homeostasis during cell cycle progression. 2018;1–27.

16. Sveiczer a, Novak B, Mitchison JM. The size control of fission yeast revisited. J Cell Sci [Internet]. 1996 Dec;109 (Pt 1:2947–57. Available from: http://www.ncbi.nlm.nih.gov/pubmed/9013342

17. Turner JJ, Ewald JC, Skotheim JM. Cell Size Control in Yeast. Curr Biol [Internet]. 2012 May [cited 2012 May 7];22(9):R350–9. Available from: http://linkinghub.elsevier.com/retrieve/pii/S0960982212001923

18. Zatulovskiy E, Skotheim JM. On the Molecular Mechanisms Regulating Animal Cell Size Homeostasis. Trends Genet [Internet]. 2020;36(5):360–72. Available from: https://doi.org/10.1016/j.tig.2020.01.011

19. Neurohr GE, Terry RL, Lengefeld J, Bonney M, Brittingham GP, Moretto F, et al. Excessive Cell Growth Causes Cytoplasm Dilution And Contributes to Senescence. Cell [Internet]. 2019 Feb;176(5):1083-1097.e18. Available from: http://www.ncbi.nlm.nih.gov/pubmed/30739799

20. Si F, Le Treut G, Sauls JT, Vadia S, Levin PA, Jun S. Mechanistic Origin of Cell-Size Control and Homeostasis in Bacteria. Curr Biol [Internet]. 2019;29(11):1760-1770.e7. Available from: https://doi.org/10.1016/j.cub.2019.04.062

21. Zlotek-Zlotkiewicz E, Monnier S, Cappello G, Le Berre M, Piel M. Optical volume and mass measurements show that mammalian cells swell during mitosis. J Cell Biol [Internet]. 2015;211(4):765–74. Available from: http://jcb.rupress.org/content/211/4/765.abstract

22. Cooper KL, Oh S, Sung Y, Dasari RR, Kirschner MW, Tabin CJ. Multiple phases of chondrocyte enlargement underlie differences in skeletal proportions. Nature [Internet]. 2013 Mar 13 [cited 2013 Mar 14];495(7441):375–8. Available from: http://www.nature.com/doifinder/10.1038/nature11940

23. Son S, Kang JH, Oh S, Kirschner MW, Mitchison TJ, Manalis S. Resonant microchannel volume and mass measurements show that suspended cells swell during mitosis. J Cell Biol [Internet]. 2015;211(4):757–63. Available from: http://www.jcb.org/cgi/doi/10.1083/jcb.201505058

24. Venkova L, Vishen AS, Lembo S, Srivastava N, Duchamp B, Ruppel A, et al. A mechano-osmotic feedback couples cell volume to the rate of cell deformation. bioRxiv [Internet]. 2021;2021.06.08.447538. Available from: https://doi.org/10.1101/2021.06.08.447538%0Ahttps://www.biorxiv.org/content/10.1101/2021.06.08.447538v2%0Ahttps://www.biorxiv.org/content/10.1101/2021.06.08.447538v2.abstract

25. Zangle TA, Teitell MA. Live-cell mass profiling: an emerging approach in quantitative biophysics. Nat Methods [Internet]. 2014;11(12):1221–8. Available from:

http://www.nature.com/doifinder/10.1038/nmeth.3175

26. Popescu G, Park K, Mir M, Bashir R. New technologies for measuring single cell mass. Lab Chip. 2014;14(4):646–52.

27. Son S, Tzur A, Weng Y, Jorgensen P, Kim J, Kirschner MW, et al. Direct observation of mammalian cell growth and size regulation. Nat Methods [Internet]. 2012 Sep [cited 2012 Nov 5];9(9):910–2. Available from: http://www.ncbi.nlm.nih.gov/pubmed/22863882

28. Liu X, Oh S, Peshkin L, Kirschner MW. Computationally enhanced quantitative phase microscopy reveals autonomous oscillations in mammalian cell growth. Proc Natl Acad Sci [Internet]. 2020 Nov 3;117(44):27388–99. Available from: http://www.pnas.org/lookup/doi/10.1073/pnas.2002152117

29. Huh D, Paulsson J. Random partitioning of molecules at cell division. Proc Natl Acad Sci. 2011;108(36):15004–9.

30. Sung Y, Tzur A, Oh S, Choi W, Li V, Dasari RR, et al. Size homeostasis in adherent cells studied by synthetic phase microscopy. Proc Natl Acad Sci U S A [Internet]. 2013 Oct 8 [cited 2014 Mar 21];110(41):16687–92. Available from: http://www.ncbi.nlm.nih.gov/pubmed/24065823

31. Fry DW, Harvey PJ, Keller PR, Elliott WL, Meade M, Trachet E, et al. Specific inhibition of cyclin-dependent kinase 4/6 by PD 0332991 and associated antitumor activity in human tumor xenografts. Mol Cancer Ther [Internet]. 2004 Nov;3(11):1427–38. Available from: http://www.ncbi.nlm.nih.gov/pubmed/15542782

32. Blajeski AL, Phan VA, Kottke TJ, Kaufmann SH. G(1) and G(2) cell-cycle arrest following microtubule depolymerization in human breast cancer cells. J Clin Invest [Internet]. 2002 Jul;110(1):91–9. Available from: http://www.ncbi.nlm.nih.gov/pubmed/12093892

33. Kafri R, Levy J, Ginzberg MB, Oh S, Lahav G, Kirschner MW. Dynamics extracted from fixed cells reveal feedback linking cell growth to cell cycle. Nature [Internet]. 2013 Feb 27 [cited 2013 Feb 27];494(7438):480–3. Available from: http://www.nature.com/doifinder/10.1038/nature11897

34. Sakaue-Sawano A, Kurokawa H, Morimura T, Hanyu A, Hama H, Osawa H, et al. Visualizing spatiotemporal dynamics of multicellular cell-cycle progression. Cell [Internet]. 2008 Feb 8 [cited 2013 Feb 10];132(3):487–98. Available from: http://www.ncbi.nlm.nih.gov/pubmed/18267078

35. Bajar BT, Lam AJ, Badiee RK, Oh YH, Chu J, Zhou XX, et al. Fluorescent indicators for simultaneous reporting of all four cell cycle phases. Nat Methods. 2016;13(12):993–6.

36. McGarry TJ, Kirschner MW. Geminin, an inhibitor of DNA replication, is degraded during mitosis. Cell. 1998;93(6):1043–53.

37. Whitfield M, Zheng L, Baldwin A, Ohta T, Hurt M, Marzluff W. Stem-loop binding protein, the protein that binds the 3′ end of histone mRNA, is cell cycle regulated by both translational and posttranslational mechanisms. … Cell Biol [Internet]. 2000 [cited 2014 Jan 15];20:4188–98. Available from: http://mcb.asm.org/content/20/12/4188.short

38. Burnham, Kenneth P., Anderson DR. Model Selection and Multimodel Inference [Internet]. Burnham KP, Anderson DR, editors. New York, NY: Springer New York; 2004. Available from: http://link.springer.com/10.1007/b97636

39. Godin M, Delgado FF, Son S, Grover WH, Bryan AK, Tzur A, et al. Using buoyant mass to measure the growth of single cells. Nat Methods [Internet]. 2010 [cited 2013 Jan 10];7(5):387–90. Available from: http://www.nature.com/nmeth/journal/vaop/ncurrent/full/nmeth.1452.html

40. Mu L, Kang JH, Olcum S, Payer KR, Calistri NL, Kimmerling RJ, et al. Mass measurements during lymphocytic leukemia cell polyploidization decouple cell cycle- And cell size-dependent growth. Proc Natl Acad Sci U S A [Internet]. 2020 Jul 7;117(27):15659–65. Available from: http://biorxiv.org/cgi/content/short/2019.12.17.879080v1?rss=1&utm_source=researcher_app&utm_medium=referral&utm_campaign=RESR_MRKT_Researcher_inbound

41. Liu S, Tan C, Melo-gavin C, Mark KG, Ginzberg MB, Blutrich R, et al. Large cells activate global protein degradation to maintain cell size homeostasis. bioRxiv. 2021;1–31.

42. Miettinen TP, Kang JH, Yang LF, Manalis SR. Mammalian cell growth dynamics in mitosis. Elife. 2019;8:1–29.

43. Ghenim L, Allier C, Obeid P, Hervé L, Fortin J-Y, Balakirev M, et al. A new ultradian rhythm in mammalian cell dry mass observed by holography. Sci Rep [Internet]. 2021;11(1):1–12. Available from: https://doi.org/10.1038/s41598-020-79661-9

44. Laplante M, Sabatini DM. mTOR signaling in growth control and disease. Cell [Internet]. 2012 Apr 13 [cited 2014 Jul 9];149(2):274–93. Available from: http://www.pubmedcentral.nih.gov/articlerender.fcgi?artid=3331679&tool=pmcentrez&rendertype=abstract

45. Ruvinsky I, Sharon N, Lerer T, Cohen H, Stolovich-Rain M, Nir T, et al. Ribosomal protein S6 phosphorylation is a determinant of cell size and glucose homeostasis. Genes Dev. 2005;19(18):2199–211.

46. Ginzberg MB. Size control and uniformity in animal cells. Harvard University; 2015.

47. Li J, Kim SG, Blenis J. Rapamycin: One drug, many effects. Cell Metab [Internet]. 2014;19(3):373–9. Available from: http://dx.doi.org/10.1016/j.cmet.2014.01.001

48. Alberts B, Johnson A, Lewis J, Raff M, Roberts K, Walter P. Molecular biology of the cell. Garland Science, Taylor & Francis Group; 2008.

49. Wullschleger S, Loewith R, Hall MN. TOR signaling in growth and metabolism. Cell [Internet]. 2006 Feb 10 [cited 2012 Oct 28];124(3):471–84. Available from: http://www.ncbi.nlm.nih.gov/pubmed/16469695

50. Zhang Y, Nicholatos J, Dreier JR, Ricoult SJH, Widenmaier SB, Hotamisligil GS, et al. Coordinated regulation of protein synthesis and degradation by mTORC1. Nature [Internet]. 2014;513(7518):440–3. Available from: http://www.nature.com/doifinder/10.1038/nature13492

51. Schneider-Poetsch T, Ju J, Eyler DE, Dang Y, Bhat S, Merrick WC, et al. Inhibition of eukaryotic translation elongation by cycloheximide and lactimidomycin. Nat Chem Biol [Internet]. 2010 Mar;6(3):209–17. Available from: http://www.ncbi.nlm.nih.gov/pubmed/20118940

52. Lee DH, Goldberg AL. Proteasome inhibitors: valuable new tools for cell biologists. Trends Cell Biol [Internet]. 1998 Oct;8(10):397–403. Available from: http://www.ncbi.nlm.nih.gov/pubmed/9789328

53. Lin J, Amir A. Homeostasis of protein and mRNA concentrations in growing cells. Nat Commun [Internet]. 2018 Dec 29;9(1):4496. Available from: https://www.biorxiv.org/content/early/2018/01/29/255950

54. Taubenberger A V., Baum B, Matthews HK. The Mechanics of Mitotic Cell Rounding. Front Cell Dev Biol. 2020;8(August):1–16.

55. Voldner N, Frey Frøslie K, Godang K, Bollerslev J, Henriksen T. Determinants of birth weight in boys and girls. human_ontogenetics [Internet]. 2009 Mar 18;3(1):7–12. Available from: https://onlinelibrary.wiley.com/doi/10.1002/huon.200900001

56. Amir A. Is cell size a spandrel? Elife. 2017;6:1–8.

57. Björklund M. Cell size homeostasis: Metabolic control of growth and cell division. Biochim Biophys Acta - Mol Cell Res [Internet]. 2019 Mar;1866(3):409–17. Available from: https://doi.org/10.1016/j.bbamcr.2018.10.002

58. Chen Y, Futcher B. Scaling gene expression for cell size control and senescence in Saccharomyces cerevisiae. Current Genetics. Springer Science and Business Media Deutschland GmbH; 2020.

59. Harris LK, Theriot JA. Relative rates of surface and volume synthesis set bacterial cell size. Cell. 2016;165(6):1479–92.

60. Rishal I, Kam N, Perry RBT, Shinder V, Fisher EMCC, Schiavo G, et al. A Motor-Driven Mechanism for Cell-Length Sensing. Cell Rep [Internet]. 2012;1(6):608–16. Available from: http://dx.doi.org/10.1016/j.celrep.2012.05.013

61. Ma XM, Blenis J. Molecular mechanisms of mTOR-mediated translational control. Nat Rev Mol Cell Biol [Internet]. 2009 May [cited 2013 Jan 28];10(5):307–18. Available from: http://www.ncbi.nlm.nih.gov/pubmed/19339977

62. Saxton RA, Sabatini DM. mTOR Signaling in Growth, Metabolism, and Disease. Vol. 168, Cell. Cell Press; 2017. p. 960–76.

63. Turner JJ, Ewald JC, Skotheim JM. cell size control in yeast. Curr Biol. 2012;29(6):997–1003.

64. Navarro FJ, Nurse P. A systematic screen reveals new elements acting at the G2/M cell cycle control. Genome Biol. 2012;13(5).

65. Keifenheim D, Sun XM, D'Souza E, Ohira MJ, Magner M, Mayhew MB, et al. Size-Dependent Expression of the Mitotic Activator Cdc25 Suggests a Mechanism of Size Control in Fission Yeast. Curr Biol [Internet]. 2017;27(10):1491-1497.e4. Available from: http://dx.doi.org/10.1016/j.cub.2017.04.016

66. Donzelli M, Draetta GF. Regulating mammalian checkpoints through Cdc25 inactivation. EMBO Rep. 2003;4(7):671–7.

67. Zhao RY, Elder RT. Viral infections and cell cycle G2/M regulation. Cell Res. 2005;15(3):143–9.

68. Gemble S, Bernhard SV, Srivastava N, Wardenaar R, Nano M, Macé A-S, et al. Mechanisms of genetic instability in a single S-phase following whole genome doubling. bioRxiv [Internet]. 2021;2021.07.16.452672. Available from: https://www.biorxiv.org/content/10.1101/2021.07.16.452672v1%0Ahttps://www.biorxiv.org/content/10.1101/2021.07.16.452672v1.abstract

69. Mei L, Cook JG. Efficiency and equity in origin licensing to ensure complete DNA replication. Biochem Soc Trans [Internet]. 2021 Nov 1;49(5):2133–41. Available from: https://portlandpress.com/biochemsoctrans/article/49/5/2133/229829/Efficiency-and-equity-in-origin-licensing-to

70. Maya-Mendoza A, Moudry P, Merchut-Maya JM, Lee M, Strauss R, Bartek J. High speed of fork progression induces DNA replication stress and genomic instability. Nature [Internet]. 2018;559(7713):279–84. Available from: http://dx.doi.org/10.1038/s41586-018-0261-5

71. Arora M, Moser J, Phadke H, Basha AA, Spencer SL. Endogenous Replication Stress in Mother Cells Leads to Quiescence of Daughter Cells. Cell Rep [Internet]. 2017;19(7):1351–64. Available from: http://dx.doi.org/10.1016/j.celrep.2017.04.055

72. Jun S, Taheri-Araghi S. Cell-size maintenance: universal strategy revealed. Trends Microbiol [Internet]. 2015;23(1):4–6. Available from: http://linkinghub.elsevier.com/retrieve/pii/S0966842X14002455

73. Si F, Le Treut G, Sauls JT, Vadia S, Levin PA, Jun S. Mechanistic Origin of Cell-Size Control and Homeostasis in Bacteria. Curr Biol. 2019;29(11):1760-1770.e7.

74. Wallden M, Fange D, Lundius EG, Baltekin Ö, Elf J. The Synchronization of Replication and Division Cycles in Individual E. coli Cells. Cell. 2016;166(3):729–39.

75. Soifer I, Barkai N. Systematic identification of cell size regulators in budding yeast. Mol Syst Biol [Internet]. 2014;10:761. Available from: http://www.pubmedcentral.nih.gov/articlerender.fcgi?artid=4299602&tool=pmcentrez&rendertype=abstract

76. Di Talia S, Skotheim JM, Bean JM, Siggia ED, Cross FR, Talia S Di, et al. The effects of molecular noise and size control on variability in the budding yeast cell cycle. Nature [Internet]. 2007 Aug 23 [cited 2012 Feb 29];448(7156):947–51. Available from: http://www.ncbi.nlm.nih.gov/pubmed/17713537

77. Yang X, Lau K-Y, Sevim V, Tang C. Design principles of the yeast G1/S switch. PLoS Biol [Internet]. 2013 Oct [cited 2013 Oct 22];11(10):e1001673. Available from: http://www.pubmedcentral.nih.gov/articlerender.fcgi?artid=3794861&tool=pmcentrez&rendertype=abstract

78. Chandler-Brown D, Schmoller KM, Winetraub Y, Skotheim JM. The Adder Phenomenon Emerges from Independent Control of Pre- and Post-Start Phases of the Budding Yeast Cell Cycle. Curr Biol [Internet]. 2017;27(18):2774-2783.e3. Available from: http://dx.doi.org/10.1016/j.cub.2017.08.015

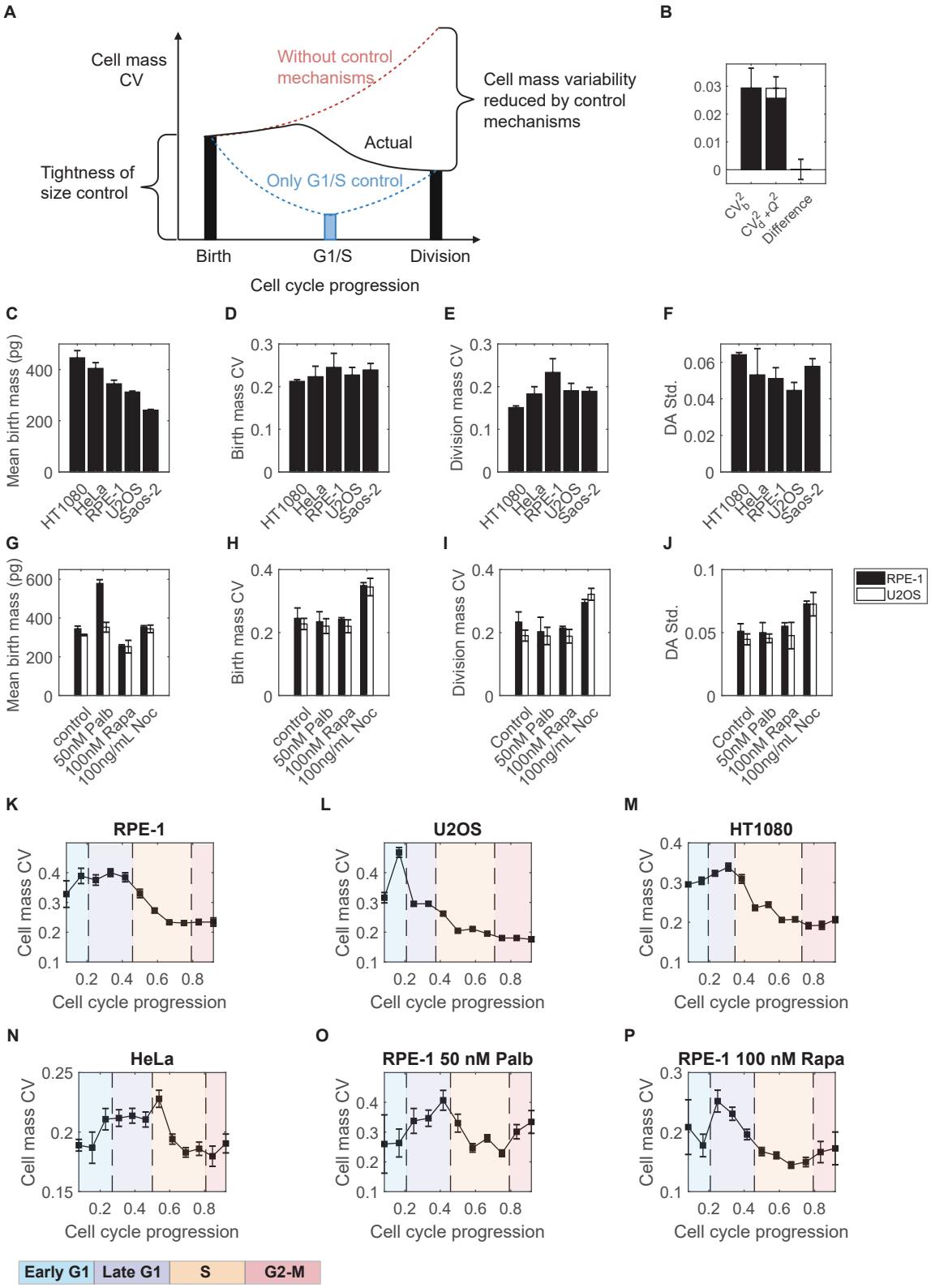
A
Cell mass CV
Without control mechanisms
Cell mass variability reduced by control mechanisms
Actual
Tightness of size control
Only G1/S control
Birth
G1/S
Division
Cell cycle progression
B
0.03
0.02
0.01
0
CV_b^2
$CV_d^2+Q^2$
Difference
C
Mean birth mass (pg)
400
200
0
HT1080
HeLa
RPE-1
U2OS
Saos-2
D
Birth mass CV
0.3
0.2
0.1
0
E
Division mass CV
F
DA Std.
0.06
0.04
0.02
G
600
H
I
J
RPE-1
U2OS
control
50nM Palb
100nM Rapa
100ng/mL Noc
K
RPE-1
L
U2OS
M
HT1080
Cell mass CV
0.4
0.3
0.2
0.1
0.2
0.4
0.6
0.8
Cell cycle progression
N
HeLa
0.25
0.15
O
RPE-1 50 nM Palb
P
RPE-1 100 nM Rapa
Early G1
Late G1
S
G2-M

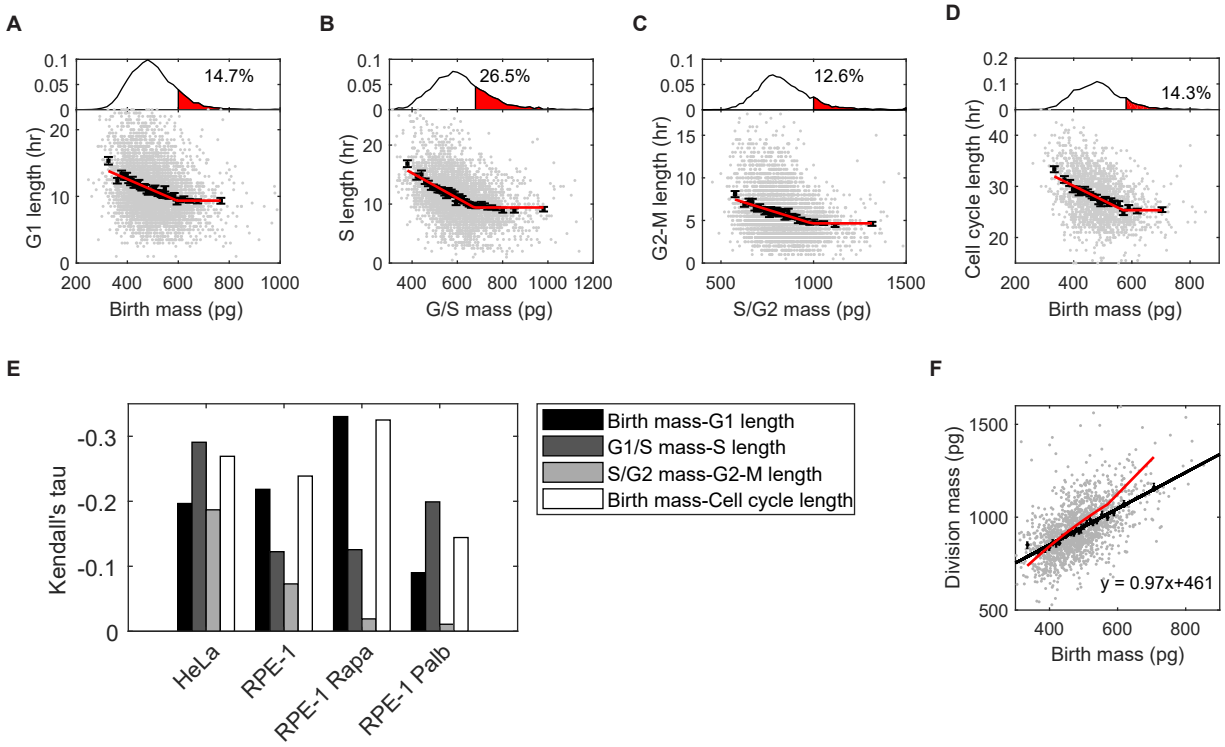
A
14.7%
G1 length (hr)
Birth mass (pg)
B
26.5%
S length (hr)
G/S mass (pg)
C
12.6%
G2-M length (hr)
S/G2 mass (pg)
D
14.3%
Cell cycle length (hr)
Birth mass (pg)
E
Kendall's tau
HeLa
RPE-1
RPE-1 Rapa
RPE-1 Palb
Birth mass-G1 length
G1/S mass-S length
S/G2 mass-G2-M length
Birth mass-Cell cycle length
F
Division mass (pg)
y = 0.97x+461
Birth mass (pg)

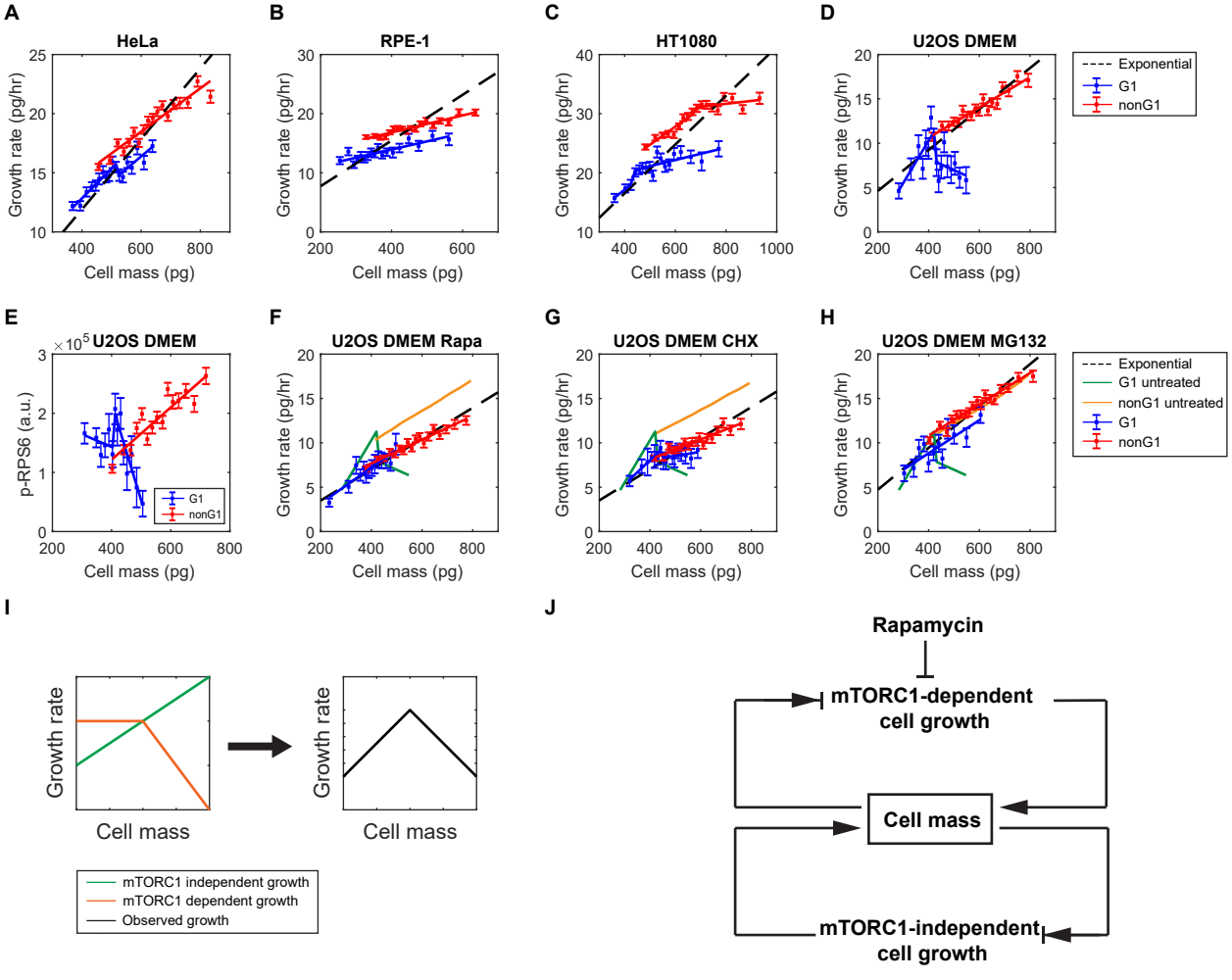
A
HeLa
Growth rate (pg/hr)
Cell mass (pg)
B
RPE-1
C
HT1080
D
U2OS DMEM
Exponential
G1
nonG1
E
U2OS DMEM
p-RPS6 (a.u.)
F
U2OS DMEM Rapa
G
U2OS DMEM CHX
H
U2OS DMEM MG132
Exponential
G1 untreated
nonG1 untreated
G1
nonG1
I
Growth rate
Cell mass
mTORC1 independent growth
mTORC1 dependent growth
Observed growth
J
Rapamycin
mTORC1-dependent cell growth
Cell mass
mTORC1-independent cell growth

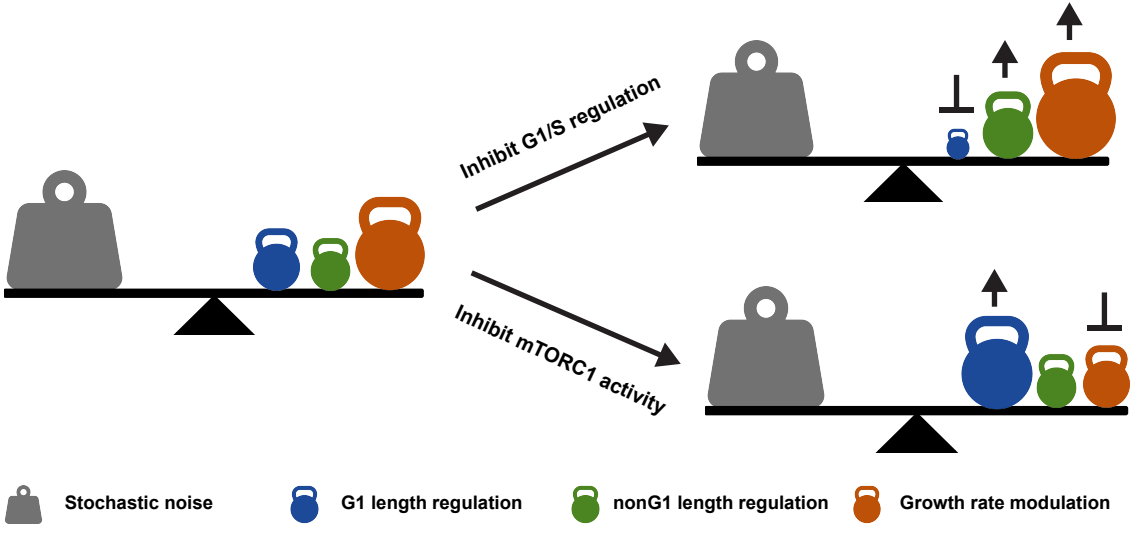
Inhibit G1/S regulation
Inhibit mTORC1 activity
Stochastic noise
G1 length regulation
nonG1 length regulation
Growth rate modulation